



## PAPER

## High-temperature resistant polypropylene films enhanced by atomic layer deposition

## OPEN ACCESS

## RECEIVED

3 December 2020

## REVISED

27 January 2021

## ACCEPTED FOR PUBLICATION

10 February 2021

## PUBLISHED

19 February 2021

Original content from this work may be used under the terms of the [Creative Commons Attribution 4.0 licence](#).

Any further distribution of this work must maintain attribution to the author(s) and the title of the work, journal citation and DOI.



Xudong Wu, Shaokai Tang, Guanghui Song, Zihan Zhang and Daniel Q Tan

Technion Israel Institute of Technology and Guangdong Technion Israel Institute of Technology, 241 Daxue Road, Shantou, 515063, People's Republic of China

E-mail: [daniel.tan@gtiit.edu.cn](mailto:daniel.tan@gtiit.edu.cn)**Keywords:** polypropylene, high temperature stability, dielectric strength, atomic layer depositionSupplementary material for this article is available [online](#)**Abstract**

Last two decades has witnessed various technical programs towards the development of new dielectric films for high temperature and high energy density capacitor technology. Yet, the organic polypropylene film still holds its top position for film capacitors required for electric and electronic power applications such as power grid, hybrid electric vehicles, oil and gas exploration, and aviation. However, its low temperature stability determined by its structural nature limits its further adoption for more rising markets. This work thus developed a creative method (ultrathin coating of inorganic compound using atomic layer deposition) to increase the high temperature stability and the dielectric strength of such a strategically important polymer film from below 105 °C to above 140 °C. Several techniques also confirmed the effective minimization of the dimensional change and crystallinity loss at higher temperatures, i.e., Thermomechanical analysis, Dynamic mechanical analysis, Dynamic Scanning calorimetry, x-ray diffraction and electron microscopy techniques. This breakthrough discovery adds a huge value to the commercial PP films and relevant capacitor industry and will extend the operation of high-performance PP film capacitors to various high standard applications.

**1. Introduction**

Polypropylene (PP) has become the low-cost and important polymeric material indispensable for the modern world. Besides being used for water/air purification, healthcare/medical device, and battery separators, PP dense films also play an important role in the electrical insulation and energy storage capacitors, food industry, and packaging industry [1–3]. Its functionalization and composite engineering further benefit the engineering plastics industry [4, 5]. A striking fact in the past 65 years is the dominant position of PP films in the capacitor industry for its superior dielectric strength, low dielectric loss and moisture intake, partial crystallinity, and mature processibility in mass production of thin films. PP film capacitors possessing a high operation voltage, a short time constant, and a long service life have become the top choice for various electrical and electronic applications such as power electronics, electric vehicles, petroleum exploration, aerospace, power transmission and distribution, and pulsed power weapons [6, 7]. However, the PP films are subject to a lower operating temperature because of large dimensional changes and lower voltage withstanding capabilities at higher temperatures higher than 105 °C [8, 9]. The current PP films cannot meet the rising needs for the high temperature applications. Therefore, various efforts turned to explore high temperature polymers to replace PP dielectric over the last two decades, yet nothing can be claimed successful for different concerns [10, 11]. For instance, Polytetrafluoroethylene (PTFE) stands out as a right candidate (so-called high temperature version of PP dielectric); however, subjects to higher cost, low yield, and scale-up manufacturing issue [12].

Meanwhile, limited researchers tried to increase the dielectric constant or energy density of PP films by changing the functional groups of its molecular chain or original resins. However, these approaches suffer from increased dielectric loss, cost, and process difficulty in the resin and film processes [13, 14]. Although filling PP

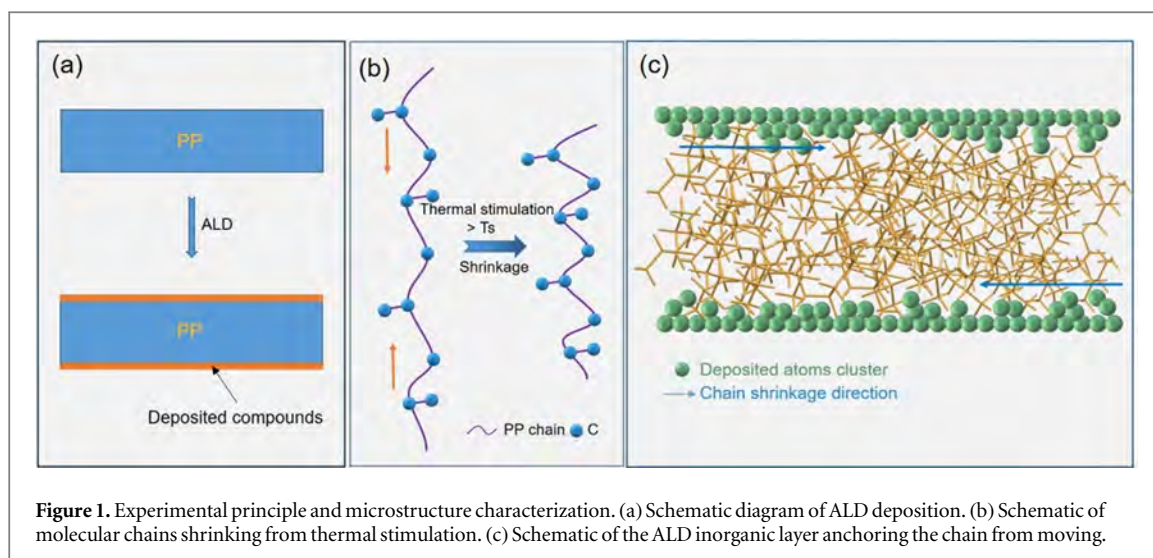


**Figure 1.** Experimental principle and microstructure characterization. (a) Schematic diagram of ALD deposition. (b) Schematic of molecular chains shrinking from thermal stimulation. (c) Schematic of the ALD inorganic layer anchoring the chain from moving.

with inorganic powders or fibers attempts to increase the mechanical strength and glass transition temperature, it would always sacrifice the flexibility and withstand-voltage capability at the same time. Such a composite engineering approach is practically tricky in manufacturing because of the marked reduction in the mechanical flexibility and dielectric strength for films thinner than 5 microns [15, 16]. The most effective method to improve the dielectric properties of PP films remains to be the biaxial stretching, a traditional scalable technique which improves the crystallinity and orientation of PP film to 60%–70% [17, 18]. Nevertheless, the room for further improvement is minimal and ~30% of microstructure still remains in an amorphous state or short-range order. Before better PP resins and processes come into play for a drastic situational change, it makes more sense to re-visit the commercially available PP films and enhance their high thermal stability and electrical performance. Pushing its operation temperatures to 125 °C or higher will revolutionize the PP film capacitor technology, meet much more stringent standards, and increase the market share by billions of US dollars.

To address the issues of dimensional instability and the lowered breakdown strength of PP films at high temperatures, the authors provide a fundamental insight into the design of PP film surface coating to enable the atomic level constraint of molecular chain movement, which would stabilize amorphous phase, crystalline orientation, and the possible electrical charges. This concept has the basis of the evidence of the increased glass transition temperature ( $T_g$ ) or operating temperature of a polymer filled with nanoparticles [19, 20]. The authors envisage the use of atomic layer deposition technique to coat an ultra-thin layer of metal oxide or nitride conform to the underlined molecular chains of the commercial PP films (i.e., to increase the ‘inertness’). The key idea behind this is to maintain the crystalline orientation of biaxially oriented PP (BOPP) through an external confinement of the molecular chains of both amorphous phase and crystalline phases at the interface. ALD is different from the physical vapor deposition (PVD) and chemical vapor deposition (CVD) processes, where large particles form in the chamber before landing on the substrate surface, leading to rough physical contact in microscopic length scale. ALD alternately deposits precursor atoms on the film surface, forming the target inorganic compounds on an atomic scale (figure 1(a)) [21]. The atoms deposited onto the surface pits, peaks, and valleys bond closely to the PP molecular chain with a fine control of coating thickness and conformity (figures S1 and S2, supporting information (available online at [stacks.iop.org/NANOX/2/010025/mmedia](https://stacks.iop.org/NANOX/2/010025/mmedia))) [22]. As shown in figure 1(b), the molecular chains of particularly low-melting point phases tend to move at higher temperatures, resulting in the increased mobility of the molecular chains of the crystalline phases. If an external force is exerted to restrain the molecular chain’s movement, the dimensional change can be reduced in principle. At elevated temperatures, the interfacial bonding tends to ‘pull back’ the activated molecular chains and thus prohibit the loss of crystalline orientation. The ALD inorganic coating can play such a confinement role to the highly mobile chains particularly within the low-temperature amorphous regions. The conformal coating and significant hindrance from the bonding between the inorganic atomic array and the molecular chains would minimize the dimensional change caused by the thermal stimulation of  $170 \times 10^{-6}/^{\circ}\text{C}$  and internal stress release stored in the BOPP (figure 1(c)).

## 2. Experimental section

### 2.1. Materials and experimental

ALD on the PP films were done using a benchtop GEMSTAR TX ALD system (Arradiance Inc., Sudbury, MA USA) with automated control to the alternate precursor pulsing and inert gas purging steps. Argon gas was used

as carrier and purging gases and flowed into the ALD chamber with 10 sccm flow rate. The ALD chamber was pumped to 254 mTorr vacuum and heated to 90~100 °C before ALD starts. Trimethyl aluminum (TMA) and H<sub>2</sub>O served as Al and O precursors, respectively during the ALD of Al<sub>2</sub>O<sub>3</sub>. Diethyl zinc (DEZ) and H<sub>2</sub>O were used as precursors of Zn and O, respectively, during the ALD of ZnO. TMA and triethylamine (TEA) were used as precursors of Al and N, respectively during the ALD of AlN. Each precursor was kept at room temperature. Precursors TMA, TEA, and DEZ were supplied by Nanjing Ai Mou Yuan Scientific Equipment Co., Ltd with 99.99% purity. H<sub>2</sub>O as a precursor was obtained from GTIIT water pure water system. The PP and HCPP films were obtained from our sponsor companies. The PP films and precursors were used as received without any pretreatment. Al<sub>2</sub>O<sub>3</sub> nanolayer on PP was deposited at 90 °C, with each cycle dosed TMA pulse/argon flushing/H<sub>2</sub>O pulse/argon flushing for the period of 21 ms, 6 s, 21 ms, and 6 s, respectively. ZnO nanolayer on PP was deposited at 90 °C, after 400 cycles of DEZ pulse/argon flushing/H<sub>2</sub>O pulse/argon flushing for the period of 100 ms, 6 s, 100 ms, and 6 s, respectively. AlN nanolayer on PP was deposited at 100 °C, after 800 cycles of TMA pulse/argon flushing/TEA pulse/argon flushing = 200 ms/6 s/200 ms/6 s.

## 2.2. Characterization

Thermomechanical analysis (TMA) for each PP film was carried out using a Discovery TMA 450 Thermomechanical Analyzer (TA Instruments, USA), with the heating and cooling rates of 5 and 2 °C min<sup>-1</sup>, respectively. Dynamic mechanical analysis (DMA) was carried out using a TA Q800 DMA analyzer in stretch mode, with 10 μm vibration amplitude, 1 Hz frequency, and 5 °C min<sup>-1</sup> heating rate. Each PP film for DMA analysis was cut into stripes with 30 mm length and 5~7 mm width. The surface morphology of the PP films was investigated by ZEISS Sigma-500 (Germany) field emission scanning electron microscopy (FESEM). Transmission electron microscopy (TEM) images were captured by a JEOL JEM 2100F (Japan) instrument using 200 kV acceleration voltage. The crystallographic structures of baseline and ALD-coated PP films were explored by x-ray diffraction (XRD, Smartlab 9, by Rigaku Corporation in Japan) at 6°/min scan rate, using 150 mA current, 40 kV voltage, and copper target. Differential scanning calorimetry (DSC) tests were done using a TA Q200 Differential Scanning Calorimeter (TA Instruments, USA), under the protection of nitrogen gas, and the temperature increased from room temperature to 200 °C at 5 °C min<sup>-1</sup>. Breakdown voltage tests were done using a PK-CPE1801 Ferroelectric Polarization Loop and Dielectric Breakdown Test System (PolyK, USA) equipped with a Trek High Voltage Amplifier (Model: 610E), along with a homemade sample holder soaked inside a constant-temperature oil bath system.

## 2.3. Electrostatic simulation

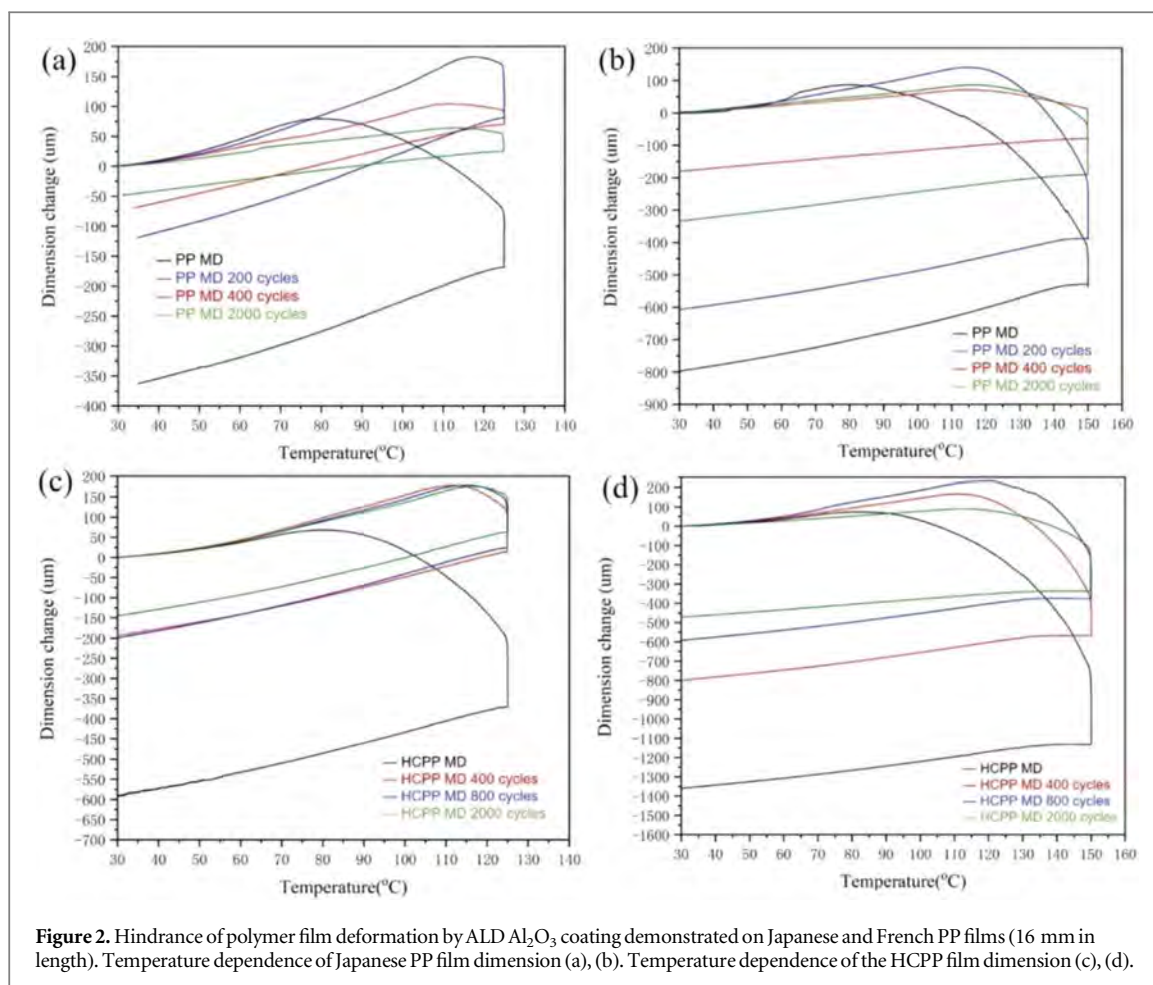
COMSOL Multiphysics 5.5 was used to simulate the distribution of electric field in x and y directions. The initial voltage of the electrode was set at 650 V. The thickness of PP and Al<sub>2</sub>O<sub>3</sub> was 1 μm and 50 nm, respectively. The ratio of dielectric constant was 1:3. The simulation results were analyzed in x-y plane.

## 3. Results and discussion

### 3.1. Film shrinkage performance

BOPP films always carry the internal stress due to the stretching operation in film manufacturing and the orientation of macromolecular chains [23]. The irreversible strain or stored potential energy of the macromolecular chains is releasable at higher temperatures resulting in the dimensional change [24]. Figure 2 illustrates this type of behavior through both Japanese PP film and French high crystallinity polypropylene (HCPP) using a Thermomechanical Analyzer TA450. When heating the PP bare film to 125 °C and 150 °C, the Machine Direction (MD) shrinkage rates show 2.3% and 5.0%, respectively, after holding for 30 min. After depositing 200-cycles ALD Al<sub>2</sub>O<sub>3</sub>, the coated film shrinks at a lower rate of 0.8% and 3.8%, respectively. With 400 cycles of Al<sub>2</sub>O<sub>3</sub>, the shrinkage rates decrease to 0.5% and 1.2% for the two temperatures. At 2000 cycles Al<sub>2</sub>O<sub>3</sub>, the shrinkage rates drop down to only 0.3% and 2.1%, respectively. The TMA study shows a turning point of about 80 °C for the PP bare film. At higher temperatures, the PP films stops expansion but turns to shrink. This transition is nothing but the contribution of stress release from the molecular chains stored in during the film stretching process. The unreleased energy remains stored in the molecular chains that require higher temperatures or longer withholding time. Additionally, we conducted multiple tests to prove the thermal stability of the coated PP films with respect to more temperature cycles, as shown in figure S3. After three heating-cooling cycles, the deformation at the elevated temperature is minimal, which shows the effectiveness of ALD coating confinement on PP film.

On the other hand, the aluminum oxide coated PP film only shrinks at a temperature as high as about 115 °C. Such enhanced dimensional stability is desirable for PP films and film capacitors to be operated at higher temperatures. Although the PP molecular chains tend to become more mobile with further increasing temperature, the oxide nanolayers' resistance limits the dimensional change of PP films down to the lower



values. Similarly, the conformal hindrance effect of the deposited inorganic coating at the molecular level is universal to other metal oxides such as  $\text{ZnO}$ ,  $\text{TiO}_2$  and  $\text{AlN}$ . After ALD treatment, these coating materials effectively limit the dimensional change of the PP films, as shown in figure S3 (supporting information). The significant increase in the working temperature ( $>30^\circ\text{C}$ ) marks a substantial industrial impact on PP film and capacitor technology and academic significance to the critical polymeric material.

### 3.2. Mechanical properties of the film

The authors used Dynamic Mechanical Analysis (DMA) to verify further the favorable role of ALD inorganic coating on stabilizing the molecular chains of low temperature phases. Figure 3(a) shows the variation of storage and loss modulus of PP films with temperature. The storage modulus of the PP bare films monotonously decreases with increasing temperature, indicating the graduation declination of its elastic strength. However,  $\text{Al}_2\text{O}_3$  coated PP films first reach the highest level at about  $63^\circ\text{C}$  and then decreases with increasing temperature in a similar way. Because of the confinement effect, the coated PP film does gain higher modulus and not subject to larger deformation at relatively lower temperatures. Therefore, the storage modulus will not drop immediately like the bare PP. But, with further increasing temperatures, the film's tension will overcome the resisting confinement of the coating layer leading to the loss of the modulus. Yet, the absolute value of the coated PP is still higher than that of bare PP, which manifests the enhancement effect of the  $\text{Al}_2\text{O}_3$  layer. At  $120^\circ\text{C}$ , its storage modulus is 310 MPa, still much higher than that of PP bare films (190 MPa). One can anticipate the elastic modulus enhancement when introducing the rigid metal oxide layers that stabilize PP molecular chains. The loss modulus of PP bare films sharply drops below  $80^\circ\text{C}$ , showing the free expansion of the chain segments. On the other hand, the loss modulus of  $\text{Al}_2\text{O}_3$  coated PP film remains less up to  $145^\circ\text{C}$ , suggesting the hindered state of the PP chains.

### 3.3. Crystal phase transition of thin films

A partial crystalline PP may comprise of high-temperature  $\alpha$  phase ( $T_m > 185^\circ\text{C}$ ), low-temperature  $\beta$  ( $T_m > 170^\circ\text{C}$ ),  $\gamma$  (hardly formed in industrial PP), and amorphous phase ( $T_m < 120^\circ\text{C}$ ). It is the low temperature phases that initiate the mobility of the entire molecular chains. Once the movement occurs, the crystallinity and crystalline orientation exhibit the relevant changes revealed by x-ray diffraction [25].

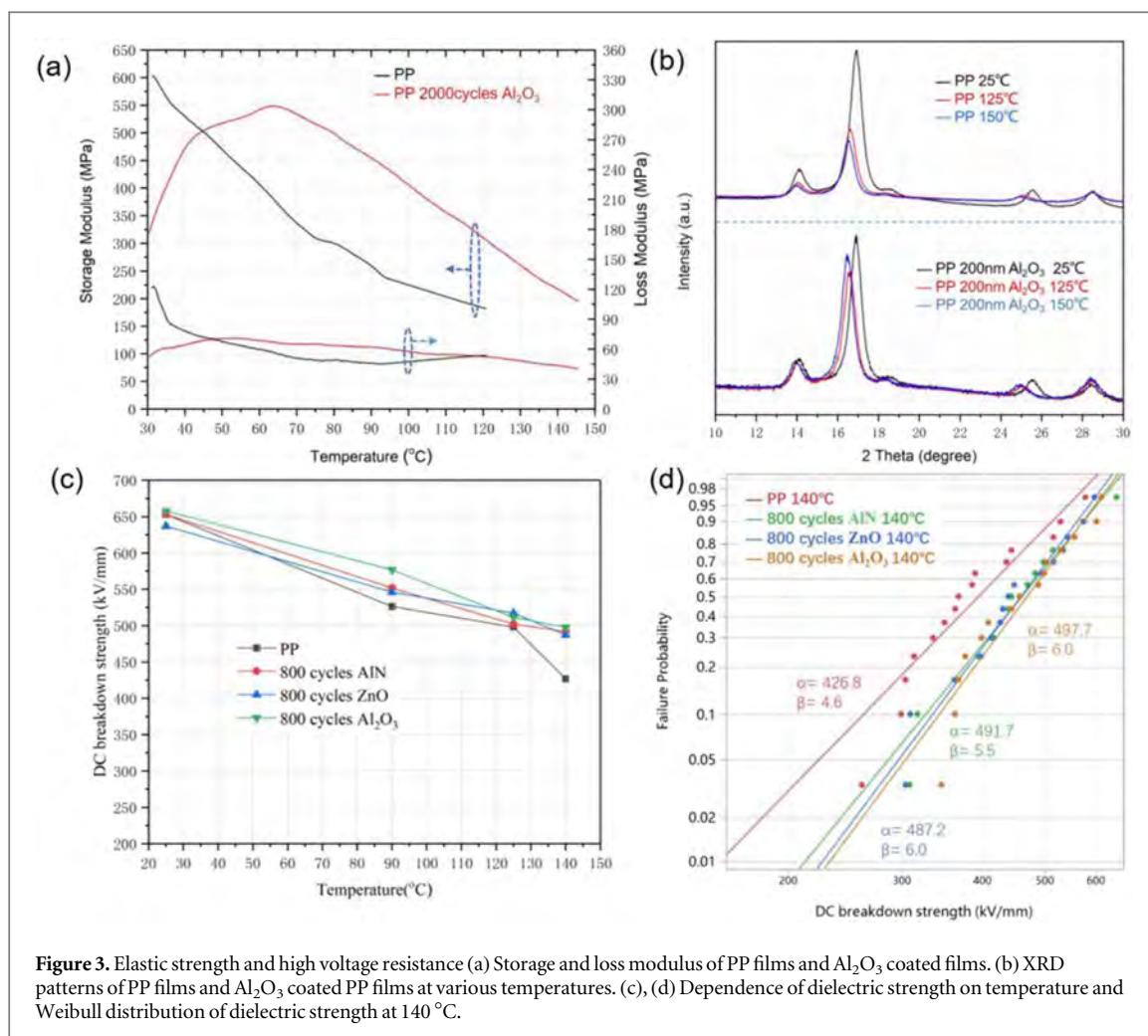


**Figure 3.** Elastic strength and high voltage resistance (a) Storage and loss modulus of PP films and Al<sub>2</sub>O<sub>3</sub> coated films. (b) XRD patterns of PP films and Al<sub>2</sub>O<sub>3</sub> coated PP films at various temperatures. (c), (d) Dependence of dielectric strength on temperature and Weibull distribution of dielectric strength at 140 °C.

Figure 3(b) shows the XRD patterns of the uncoated and Al<sub>2</sub>O<sub>3</sub> coated PP films at different temperatures. The different crystalline peaks of PP films appear at 14.1°, 17.0°, and 18.6° corresponding to the (110), (040), (130) planes of the  $\alpha$  phase, respectively [26]. The peak intensity of the PP bare films dramatically decreases with the increase of temperature. This is due to the loss of crystallinity and orientation after the low-temperature amorphous phase becomes loosened above 120 °C. In comparison, the reduction of ALD coated film peak intensity is minor, which indicates the domination of the long-range ordering of molecular structure at temperatures as high as 150 °C. This proves that the ALD inorganic coating enhances the ‘inertness’ of the molecular chains by restraining the movement of the molecular chain. Additionally, the downward shifts of the 14.1°, 17.0°, and 18.6° peaks reflect the increase in lattice parameters resulting from the release of the residual stress and the thermal expansion of the crystalline phases.

### 3.4. Thermal performance of thin films

The differences in the thermal stability and crystallization between PP films and ALD coated PP films also exhibited in Differential Scanning Calorimetry (figure S4, supporting information). The melting of the coated PP films near 170 °C starts at higher temperatures with narrower dual peaks, which implies the less mobility of molecular chains than the uncoated PP films. The large exothermic peaks of crystallization occurring around 125 °C during the cooling process are wider for the ALD coated PP films compared with the PP bare films. This difference implies the slower crystallization process in the coated PP because the ALD nanolayers may exert a conformational hindrance to the PP molecular chains. This phenomenon also presents another evidence for the enhancement mechanism of glass transition temperature or working temperature of a polymer composite system in a different way comparing with nanoparticle confinement [20].

### 3.5. Dielectric strength

Another desirable advantage of the ALD coating is the enhancement of dielectric strength of PP films in a broader temperature range. With a little higher breakdown strength, the capacitor can operate continuously at a full rated voltage with a higher voltage variation tolerance. The increased dimensional stability has set up a

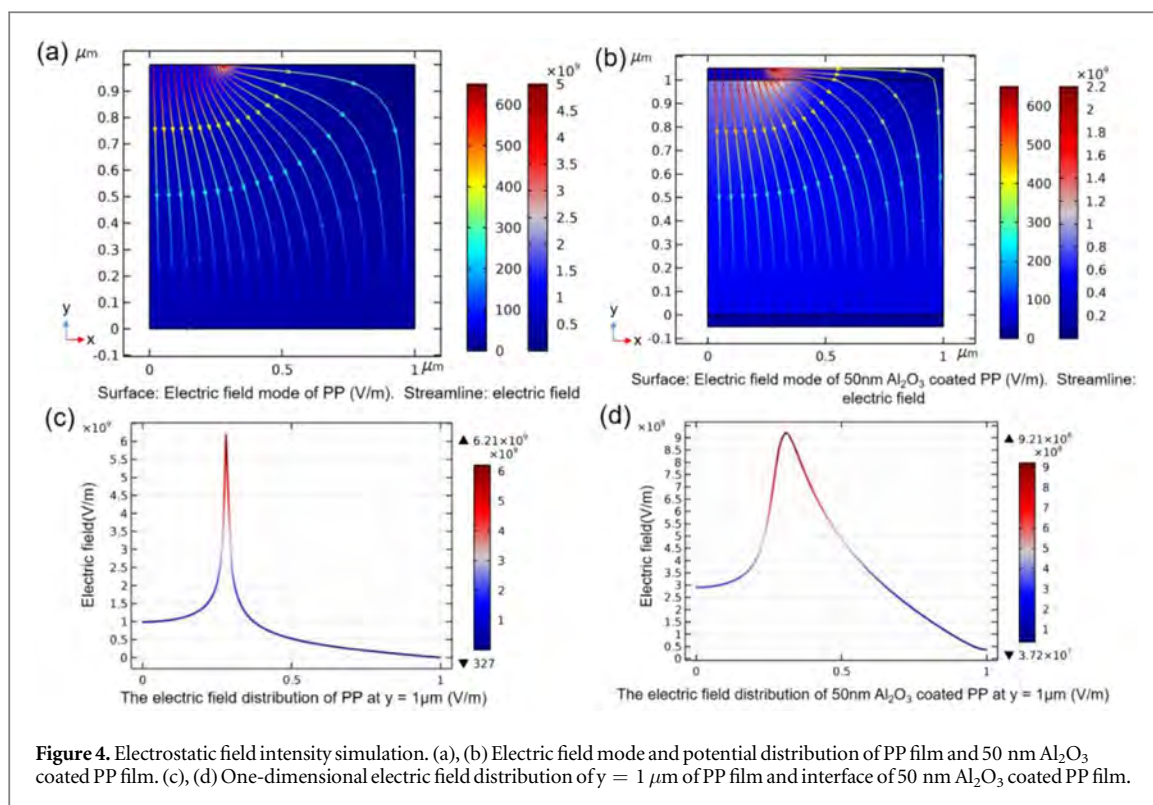


**Figure 4.** Electrostatic field intensity simulation. (a), (b) Electric field mode and potential distribution of PP film and 50 nm Al<sub>2</sub>O<sub>3</sub> coated PP film. (c), (d) One-dimensional electric field distribution of  $y = 1 \mu\text{m}$  of PP film and interface of 50 nm Al<sub>2</sub>O<sub>3</sub> coated PP film.

foundation for the coated PP films to work under high voltages at temperatures beyond 140 °C. The thermal assistance inevitably leads to a higher mobility of charge carriers generating an additional Joule heat at the working temperature. The instantaneous current flows through the breakdown sites can cause the film damage and a lowered breakdown strength [27]. The amorphous phase and other low temperature phases are the weakest links prone to such local breakdown in PP films. Stabilizing the molecular chain configuration would minimize the chain deformation and the breakdown channels, and thus push upward the breakdown voltage to higher temperatures. Figures 3(c), (d) shows DC breakdown data tested in a silicone oil bath after vacuum drying PP films (with and without ALD coating) for 3 h at 70 °C. The bare PP films subject to lowered breakdown strength (by ~35% at 140 °C) with increasing temperatures (figure S5, supporting information). The PP films coated with Al<sub>2</sub>O<sub>3</sub>, ZnO, and AlN maintain the breakdown strength of around 490 kV mm<sup>-1</sup> at 140 °C (lowered by about ~24%). Therefore, the ALD coating generates a tight bonding with the macromolecular chains and passivate the surface defects, suppressing the charge transport and thermal-assisted breakdown channels [28, 29]. The other factors in maintaining the high breakdown strength are the higher thermal conductivity of the ordered PP configuration and the coating materials (42 W mK<sup>-1</sup> for Al<sub>2</sub>O<sub>3</sub>, 60 W mK<sup>-1</sup> for ZnO, 320 W mK<sup>-1</sup> for AlN). PP has a thermal conductivity of 0.11–0.47 W mK<sup>-1</sup> depending on the structural ordering and temperatures [30]. The long-range order of the coated PP films, as revealed by XRD, can transport the heat out of the samples more effectively and give rise to higher breakdown strength at higher temperatures.

Dielectric film breakdown mechanism is an ongoing investigation that has long puzzled researchers. The dielectric phenomenon in the thin dielectric PP appears to be more related to the electrode-limited conduction mechanism that dominates at higher electric field, and temperatures [31, 32]. The most crucial parameter thus is the barrier height at the electrode-dielectric interface, unlike the bulk-limited conduction mechanisms where the trap energy level inside dielectric films matters most. The layer of a high dielectric material between the electrodes and the polymer film may increase the barrier height against the thermionic-field emission via increasing work function and charge accumulation via the weakened electric field using higher dielectric constant. The extra work function of the deposited inorganic layer in this work is a similar or a little higher than that of electrodes (i.e., 4.4 for Al, 5.1 for Au, 4.7 eV for Al<sub>2</sub>O<sub>3</sub>, 5.1 eV for ZnO, and 5.5 eV for PP) and thus not treated as serious charge barrier in this communication [33–35]. The authors only investigate the effect of the high dielectric layer such as Al<sub>2</sub>O<sub>3</sub> coating on PP film as an example to show the reduced electrostatic field distribution by COMSOL simulation. Figure S6 (supporting information) shows the cuboid PP film of 1 μm × 1 μm × 0.3 μm, where the electrode on the top is set at 0.28 × 0.3 μm. The initial potential is set at 650 V, and the dielectric constant ratio of Al<sub>2</sub>O<sub>3</sub> to PP is set at 3:1. Due to the tip discharge effect, the electric field concentrates at the edge of the electrode.

The simulation shows electric field distribution in bare and Al<sub>2</sub>O<sub>3</sub> coated PP film in figures 4(a) and (b), respectively. The magnitude of electric field intensity is critical in determining the dielectric strength of the

films. As shown in figures 4(c), (d), the one-dimensional field intensity reaches its peak value of  $6.21 \times 10^9 \text{ V m}^{-1}$  at  $y = 1 \mu\text{m}$  (interface position) before the alumina coating. The field intensity decreases to its peak value of  $9.21 \times 10^8 \text{ V m}^{-1}$  at the same interface position. The electric field lines passing through the interface in figure 4(b) are more uniform than those in figure 4(a), which means that the  $\text{Al}_2\text{O}_3$  coating weakens the charge localization or field strength compared with bare PP (figure S7, supporting information). As a result,  $\text{Al}_2\text{O}_3$  coating on PP film delays the dielectric breakdown by the weakened electric field. Particularly at higher temperatures when thermionic-field emission becomes severe, the high dielectric layer increases the charge barrier height for charge injection so as to enable the PP film operational under higher voltages.

## 4. Conclusions

In summary, this work discovers an effective method for the first time to enable the commercial polypropylene films to sustain their high-temperature operation utilizing an ALD inorganic coating. The modified polypropylene films ( $\sim 3 \mu\text{m}$ ) have a thermal resistance to temperatures as high as  $150^\circ\text{C}$ , demonstrated by minimal deformation, enhanced mechanical strength, and a high breakdown strength at high temperatures. The modified polypropylene films only require an oxide layer or nitride layer of 40–200 nm in thickness coated on the surface of the polypropylene film. The modified polypropylene film only exhibits a dimensional change of less than 0.5% and maintains a breakdown strength of  $>490 \text{ kV mm}^{-1}$  at  $140^\circ\text{C}$ , which was verified using computer modeling. The coated film flexibility and mechanical integrity are also required in the capacitor winding process and cyclic operation. The nanometer layer is minimal comparing with the PP film of several microns has not caused degradation in the limited cyclic test ( $140^\circ\text{C}$ ). The ALD-modified polypropylene film has widespread applications in film capacitors and other electronic products with high-temperature requirements.

## Acknowledgments

This work was also supported by the Guangdong Basic and Applied Basic Research Foundation—2019A1515012056 and the Guangdong-Israel Special Research Grant 200902154890781.

## Data availability statement

All data that support the findings of this study are included within the article (and any supplementary files).

## ORCID iDs

Daniel Q Tan  <https://orcid.org/0000-0002-2282-2000>

## References

- [1] Creton C 2017 *Science* **355** 797
- [2] Song G and Tan D Q 2020 *Macromol. Mater. Eng.* **305** 2000127
- [3] Liu B, Yang M, Zhou W-Y, Cai H-W, Zhong S-L, Zheng M-S and Dang Z-M 2020 *Energy Storage Mater.* **27** 443
- [4] Eagan J M, Xu J, Di Girolamo R, Thurber C M, Macosko C W, LaPointe A M, Bates F S and Coates G W 2017 *Science* **355** 814
- [5] Maddah H A 2016 *Am. J. Polym. Sci.* **6** 1
- [6] Carr S F, Adams S, Weimer J, Wu R, Kosai H, Bray K, Furmaniak T, Barshaw E, Scozzie S and Jow R 2004 *SAE transactions*. **113** 2033 ([www.jstor.org/stable/44738089](http://www.jstor.org/stable/44738089))
- [7] Tan D Q 2019 *Adv. Funct. Mater.* **30** 1808567
- [8] Ho J and Jow R July 2009 Characterization of high temperature polymer thin films for power conditioning capacitors *Army Research Lab Adelphi Md Sensors and Electron Devices Directorate* **2019** ARL-TR-4880
- [9] Rabuffi M and Picci G 2002 *IEEE Trans. Plasma Sci.* **30** 1939
- [10] Tan D, Zhang L, Chen Q and Irwin P 2014 *J. Electron. Mater.* **43** 4569
- [11] Yializis A and Taylor R S 2017 *High Temperature DC-Bus Capacitor Cost Reduction and Performance Improvements* (Tucson, AZ (United States): Sigma Technologies International Group, Inc.)
- [12] Ho S Janet and Greenbaum Steven G 2018 *ACS Applied Materials & Interfaces* **10** 29189
- [13] Chung T 2002 *Prog. Polym. Sci.* **27** 39
- [14] Zhu L 2014 *J Phys Chem Lett.* **5** 3677
- [15] Neusel C and Schneider G A 2014 *J. Mech. Phys. Solids.* **63** 201
- [16] Iniestra-Galindo M, Perez-Gonzalez J, Marin-Santibanez B and Balmori-Ramirez H 2019 *Mater. Res. Express* **6** 105347
- [17] Liu H and Huo H 2014 *Colloid Polym. Sci.* **292** 849
- [18] Nash J L 1988 *Polym. Eng. Sci.* **28** 862

- [19] Oh H-J and Green P F 2009 *Nat. Mater.* **8** 139
- [20] Roldughin V I, Serenko O A, Getmanova E V, Novozhilova N A, Nikifirova G G, Buzin M I, Chvalun S N, Ozerin A N and Muzafarov A M 2016 *Polym. Compos.* **37** 1978
- [21] George S M 2010 *Chem Rev.* **110** 111
- [22] McClure C D, Oldham C J and Parsons G N 2015 *Surf. Coat. Technol.* **261** 411
- [23] Fischer C and Drummer D 2016 *Int. J. Polym. Sci.* **2016** 1–11
- [24] Lacks D J and Rutledge G C 1994 *Chem. Eng. Sci.* **49** 2881
- [25] Segerman E and Stern P 1966 *Nature* **210** 1258
- [26] Lima M F S, Vasconcellos M A Z and Samios D 2002 *J. Polym. Sci., Part B: Polym. Phys.* **40** 896
- [27] Ho J and Jow T R 2012 *IEEE Trans. Dielectr. Electr. Insul.* **19** 990–5
- [28] Tan D Q 2020 *IET Nanodielectr.* **3** 28
- [29] Zhou Y, Li Q, Dang B, Yang Y, Shao T, Li H, Hu J, Zeng R, He J and Wang Q 2018 *Adv. Mater.* **30** 1805672
- [30] Patti A and Acierno D 2019 *Polypropylene-Polymerization and Characterization of Mechanical and Thermal Properties* (Weiyu Wang and Yiming Zeng: IntechOpen) (<https://www.intechopen.com>) (<https://doi.org/10.5772/intechopen.84477>)
- [31] Tan D Q 2020 *J. Appl. Polym. Sci.* **137** 49379
- [32] Chiu F-C 2014 *Adv. Mater. Sci. Eng.* **2014** 578168
- [33] Rajopadhye N and Bhoraskar S 1986 *J. Mater. Sci. Lett.* **5** 603
- [34] Kitamura S, Suzuki K and Iwatsuki M 1999 *Appl. Surf. Sci.* **140** 265
- [35] Song W and Yoshitake M 2005 *Appl. Surf. Sci.* **251** 14